

A physical model for one-dimension and time-dependent ionosphere.

Part I. Description of the model

Shun-rong Zhang^{(1)(*)}, Xin-yu Huang⁽²⁾, Yuan-zhi Su⁽²⁾ and Sandro Maria Radicella⁽¹⁾

⁽¹⁾ International Centre for Theoretical Physics, Trieste, Italy

⁽²⁾ Wuhan Institute of Physics, Chinese Academy of Sciences, Wuhan, P.R. China

Abstract

On the basis of continuity and momentum equations for the ionospheric F region, a time-dependent and one-dimension model for O^+ , N_2^+ , O_2^+ , and NO^+ , taking into account photoionization production, 10 recombination reactions, thermospheric wind and electromagnetic drifts, has been derived. The bottom side boundary is set to be dominated by photo-chemical reactions, meanwhile, the top side can be influenced by other processes. Electron density, foF_2 , or flux can be given as input. The present model can be used for the investigation of the influence of different parameters on the ionospheric processes, such as neutral wind, solar radiation flux, electromagnetic forces, and others. This part gives the description of the model. Numerical results and its physical discussions will be addressed in the next paper.

Key words *aeronomy – ionosphere*

1. Introduction

For the recent 2 decades, ionospheric modeling has been one of the leading patterns in the study of ionospheric structure. The empirical and semi-empirical models (not discussed here) are directly relevant to observational results with little theoretical output. Theoretical models, also named first principle models (Stening, 1992) are derived from various laws of physics. In this approach, the NCAR-TIGCM (Roble *et al.*, 1988), and Utah State University Model (Sojka and Schunk, 1985), are among the most important 3-d and time-dependent ionosphere-thermosphere interactive models. However, the considerable demand for CPU time and computing memory make it

nearly impossible for these models to be utilized in computers other than supercomputers. For this reason only limited output is available for different geophysical conditions such as solar and geomagnetic activity, seasonal and local time variations.

Beside the mentioned models, many small scale models have been developed. For the low latitudes, there are Anderson's model (Anderson, 1973), Chan and Walker's model (Chan and Walker, 1984; Walker and Chan, 1989), which are all interested in EIA (Equatorial Ionization Anomaly) over America or East Asia sectors. Every model has its limitation, as pointed out by Stening (1992), and the success of a model depends on the correct choice of its input, particularly the neutral wind and electric field. Hence, at the present stage, it is important to be able to understand and to study the impact of various background parameters on the ionospheric process, like wind, electric field and solar X.U.V. radiation. This understanding is essential to the ionospheric physics itself, herewith it provides a

(*) Permanent address: Wuhan Institute of Physics, Chinese Academy of Sciences, P.O., Box 72003, Wuhan 430072, P.R. China.

guide for a more adequate computer simulation work.

2. Theoretical basis

2.1. Continuity equations

The continuity equation for O^+ may be written as:

$$\frac{\partial N_1}{\partial t} = q_1 - \beta_1 N_1 - \frac{\partial(N_1 v_z)}{\partial z} \quad (2.1)$$

where, the horizontal contribution in the transport term has been neglected in the one dimension model. N_1 , q_1 , β_1 and v_z are the density, production rate, loss rate and drift velocity respectively. Other ion species, NO^+ , N_2^+ , and O_2^+ are the major ion species in the E region and low F region where dynamic process plays a less important role, and the transport term can be ignored. Also, H^+ transport is neglected over the height range concerned. The equation for these species is given by:

$$\frac{\partial N_i}{\partial t} = q_i - \beta_i N_i \quad (2.2)$$

In the above equation, subscript « i » denotes the ion species.

2.1.1. Photoionization production rate

The photoionization production rate q_j for the j species (O^+ , or O_2^+ , or N_2^+) as a function of height z and solar zenith angle χ can be expressed as:

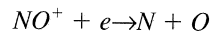
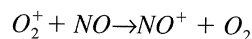
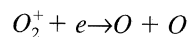
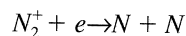
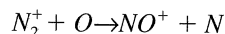
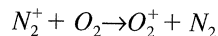
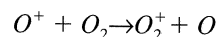
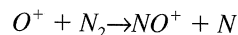
$$q_j(h, \chi) = \sum_{\lambda} F_{\infty \lambda} \exp[-\tau(z, \chi)] \sigma_{j\lambda} n_j n_{j\lambda} \quad (2.3)$$

where $F_{\infty \lambda}$ is the solar radiation flux at zero optical depth, $\tau(z, \chi)$ is the optical depth and $\sigma_{j\lambda}$, $\eta_{j\lambda}$ and n_j are, respectively, the photoionization cross-section, ionization efficiency and concentration of the j neutral species. During day-time, 77 wavelength bands are utilized

(Torr *et al.*, 1979), while night-time ionization sources for O^+ , which are considered to be mainly resonant scattering of $HeI584\text{\AA}$ and $HeII304\text{\AA}$ (Strobel and Young, 1974), are also included in the present model as a possible contribution to the night-time ionization density.

2.1.2. Recombination reactions

The loss rate is determined by the following recombination reactions



The corresponding reaction coefficients are taken from Ruster (1971).

2.2. Momentum equation

In the ionospheric F region, the movement of ions is governed by gravity, pressure gradient, air-drag and electromagnetic forces. A general formula for O^+ is as follows:

$$0 = -\nabla P_1 + N_1 m_1 \mathbf{g} + N_1 e (\mathbf{E} + \mathbf{V} \times \mathbf{B}) - N_1 \sum_n v_{1n} \mu_{1n} (\mathbf{V} - \mathbf{U}) - N_1 \sum_i v_{1i} \mu_{1i} (\mathbf{V} - \mathbf{V}_i) \quad (2.4)$$

where $n = N_2, O_2, O, \dots$ (neutral composition) and $i = N_2^+, O_2^+, NO^+, \dots$ (ion species other than O^+), vector \mathbf{V} , \mathbf{V}_i and \mathbf{U} is the velocity of O^+ , other ions and neutral wind, respectively.

For simplification, other assumptions can be made:

- $(\sum_n v_{1n} \mu_{1n} + \sum_i v_{1i} \mu_{1i})^2 \ll e^2 B^2$,
- $\frac{\partial}{\partial x}, \frac{\partial}{\partial y} = 0$

where x is in eastward, y northward and z upward.

2.3. Diffusion equation

2.3.1. Equation and coefficients

Combining Eqs. (2.1) and (2.4), we may obtain the time-dependent and one-dimension diffusion equation with respect to O^+ .

$$\frac{\partial N_1}{\partial t} = F_1 + F_2 N_1 + F_3 \frac{\partial N_1}{\partial z} + F_4 \frac{\partial^2 N_1}{\partial z^2} \quad (2.5)$$

where

$$\begin{aligned} F_1 &= q_1 + \frac{\partial}{\partial z} \left(\frac{\theta \sin^2 I}{v} \right) \\ F_2 &= 2k \frac{\sin^2 I}{v} \frac{\partial^2 T}{\partial z^2} + \\ &+ 2k \frac{\partial}{\partial z} \left(\frac{\sin^2 I}{v} \right) \frac{\partial T}{\partial z} - \frac{\partial \Pi}{\partial z} - \beta \\ F_3 &= 4k \frac{\sin^2 I}{v} \frac{\partial T}{\partial z} + 2k \frac{\partial}{\partial z} \left(\frac{\sin^2 I}{v} \right) T - \Pi \\ F_4 &= 2k \frac{\sin^2 I}{v} T \end{aligned}$$

and

$$\begin{aligned} \theta &= -N_e k T \frac{\partial}{\partial z} \left(\frac{N_1}{N_e} \right) \\ T &= (T_i + T_e)/2 \end{aligned}$$

$$\begin{aligned} \Pi &= \frac{\cos I}{B} E_x + \frac{\cos I}{eB} \mathcal{A} - \frac{\sin I \cos I}{v} \mathcal{B} + \\ &+ \frac{\sin^2 I}{v} (\mathcal{C} - mg) \end{aligned}$$

$$\begin{aligned} v &= \sum v_{1n} \mu_{1n} + \sum v_{1i} \mu_{1i} \\ \mathcal{A} &= \sum v_{1n} \mu_{1n} u_x + \sum v_{1i} \mu_{1i} v_{ix} \\ \mathcal{B} &= \sum v_{1n} \mu_{1n} u_y + \sum v_{1i} \mu_{1i} v_{iy} \\ \mathcal{C} &= \sum v_{1n} \mu_{1n} u_z + \sum v_{1i} \mu_{1i} v_{iz} \end{aligned}$$

If $v_i = v$ is assumed, the above set of coefficients may be replaced by

$$\begin{aligned} v &= \sum v_{1n} \mu_{1n} \\ \mathcal{A} &= \sum v_{1n} \mu_{1n} u_x \\ \mathcal{B} &= \sum v_{1n} \mu_{1n} u_y \\ \mathcal{C} &= \sum v_{1n} \mu_{1n} u_z \end{aligned}$$

2.3.2. Boundary condition

At the lower boundary, where the transport can be neglected, photo-chemical processes alone are assumed:

$$\frac{\partial N_j}{\partial t} = q_j - \beta_j N_j \quad (2.6)$$

where j represents the ion species.

The upper boundary condition is not so easily defined. As a rule, two types of boundary may be adopted. The first type takes the following form:

$$N_1(z, t)|_{z=Z} = N(t) \quad (2.7)$$

The second one is:

$$f \left(\frac{\partial N_1(z, t)}{\partial z}, N_1(z, t), t \right) = 0 \quad (2.8)$$

where function f can be defined assuming dif-

ferent physical considerations. For example, from the transport relation at the top, we may have:

$$N_1 v_z = -\mathcal{D} \left(\frac{\partial N_1}{\partial z} + \frac{N_1}{H_p} \right) \quad (2.9)$$

where $N_1 v_z$ is the upper boundary flux, \mathcal{D} is the diffusion coefficient and H_p the plasma scale height. Another example is at the F_2 peak height $h_m F_2$ where we have

$$\left. \frac{\partial N_1(z, t)}{\partial z} \right|_{z=h_m F_2(t)} = 0 \quad (2.10)$$

3. Numerical procedures

3.1. General principle

To solve Eq.(2.5) numerically, differentiating may be introduced,

$$\begin{aligned} \frac{\partial N_{i,k}}{\partial t} &= \frac{N(i, k) - N(i, k-1)}{\tau} \\ \frac{\partial N_{i,k}}{\partial z} &= \frac{N(i+1, k) - N(i-1, k)}{2\mathcal{L}} \\ \frac{\partial^2 N_{i,k}}{\partial z^2} &= \frac{N(i+1, k) - 2N(i, k) + N(i-1, k)}{\mathcal{L}^2} \end{aligned}$$

where i denotes time level, whereas height level will be denoted by j and τ and \mathcal{L} are the time and height intervals. This results in a well-known numerical form of the tridiagonal system shown below

$$\begin{aligned} C_1(i, k)N(i-1, k) + C_2(i, k)N(i, k) + \\ + C_3(i, k)N(i+1, k) = R(i, k-1) \end{aligned} \quad (3.1)$$

In the above equation, $C_1(i, k)$, $C_2(i, k)$, $C_3(i, k)$ and $R(i, k)$ depend on the background parameters that appear in section 2.2.1. and 2.2.2. $R(i, k)$ is related to the density N_1 as well but at the previous time level. This equation is easily solved by means of the Thomas

algorithm if boundary and initial conditions are given. First of all, let

$$N(i, k) = \alpha(i, k)N(i-1, k) + \beta(i, k) \quad (3.2)$$

where α and β are unknown. And then insert Eq.(3.2) into Eq.(3.1), followed by

$$\alpha(i, k) = - \frac{C_1(i, k)}{C_2(i, k) + C_3(i, k)\alpha(i+1, k)} \quad (3.3)$$

$$\beta(i, k) = \frac{R(i, k-1) - \beta(i+1, k)C_3(i, k)}{C_2(i, k) + C_3(i, k)\alpha(i+1, k)} \quad (3.4)$$

Hereby, $\alpha(i, k)$ and $\beta(i, k)$ have been determined formally.

Mathematically, according to Eq.(3.2), only when all the coefficients of $\alpha(i, k)$ and $\beta(i, k)$, and also lower boundary values are determined in advance, we can find N_1 at all height and time. Now, bottom boundary condition can be easily settled, the key point is how to obtain $\alpha(i, k)$ and $\beta(i, k)$ or according to Eq.(3.3) and Eq.(3.4), to obtain $\alpha(I, k)$ and $\beta(I, k)$ (I is the height level at the top) provided that the arbitrary initial values are given. Top boundary should be recommended in this case. The following section discusses this topic.

3.2. Numerical conditions at the upper boundary

1) *Density is given* – This means $N_1(i, k)|_{i=I} = n(k)$. $n(i)$, the upper boundary density is optional: a model value (e.g., IRI, International Reference Ionosphere model), or experimental data. Hence, from Eq. (3.2), the α and β may be given by

$$\alpha(I, k) = 0$$

$$\beta(I, k) = n(k)$$

In practical calculations, $f_0 F_2$ – which of course cannot be employed as the boundary

condition due to the variability of the peak height – is introduced by assuming a set of topside values that are able to reproduce or approach the experimental foF_2 . First of all, with the help of IRI or other model values at the topside boundary, foF_2 can be simulated; and then we compare the simulated foF_2 with the experimental one, and if the relative deviation is greater than 1%, we modify the topside values and re-calculate foF_2 , and repeat this procedure until the required precision is reached.

2) *Flux is given* – The numerical formation for the following relation, as already shown in Eq. (2.8),

$$\text{flux} = -\mathcal{D} \left(\frac{\partial N_1}{\partial z} + \frac{N_1}{H_p} \right)_{i=t}$$

can be expressed as follows

$$N(I, k) = l(I, k)N(I-1, k) + m(I, k) \quad (3.5)$$

where $l(I, k)$ and $m(I, k)$ are related to flux:

$$l(I, k) = \frac{H_p}{H_p + \mathcal{L}}$$

$$m(I, k) = -\text{flux} \frac{\mathcal{L} \times H_p}{(\mathcal{L} + H_p)\mathcal{D}}$$

Therefore

$$\alpha(I, k) = l(I, k)$$

$$\beta(I, k) = m(I, k)$$

4. Input background parameters

Neutral composition, temperature, wind, electrical field, and initial ion density, upper boundary values are needed. MSIS86 (Hedin, 1986) is used to produce the concentration of O , N_2 , O_2 as well as the temperature. $[NO]$ is after Mitra (1968). Thermospheric wind may be obtained from either HWM90 (Hedin *et al.*, 1991) or VSH model (Killeen *et al.*, 1987).

Height range is from 100 km through 500 km, and height and time interval is optional with the default values of 2 km and 15 min. In order to minimize the impact of initial values on the time variation of the parameter calculated, the running of the program should last 2 or more cycles (one cycle is 24 hours).

5. Summary

The model for the vertical distribution of the time-dependent ion species O^+ , N_2^+ , O_2^+ , and NO^+ , is derived by solving the continuity and momentum equations. The major relevant processes for mid-latitude ionosphere are considered, including photoionization, 10 chemical reactions, neutral wind and $\mathbf{E} \times \mathbf{B}$ drift. Upper boundary conditions are flexible, and the environmental parameters, *i.e.* solar radiation flux, wind and $\mathbf{E} \times \mathbf{B}$ may be adjusted. Therefore, in this framework, investigations of the ionospheric morphology as a function of the background variation can be carried out numerically.

Because of simplified treatment for the dynamical and photo-chemical processes in the top and bottom, regions, the present model is assumed valid within F region. At the same time, its validity cannot be extended to very low latitudes where horizontal transport contribution becomes important.

Acknowledgements

Considerable help from the Scientific Computing Group of ICTP and the Computer Division of Wuhan Institute of Physics are greatly acknowledged. This work is supported by Chinese National Natural Sciences Funds. The visit of Zhang S.-R. to ICTP was under the Federation Agreement with Wuhan Institute of Physics and as part of the research activities of the Atmospheric Physics and Radiopropagation Laboratory of ICTP. (S.-R.Z.) would like to thank Professor Abdus Salam, the International Atomic Energy Agency and UNESCO for hospitality at the International Centre for Theoretical Physics, Trieste.

REFERENCES

- ANDERSON, D.N. (1973): A theoretical study of the ionospheric F region equatorial anomaly - 1. Theory, *Planet. Space Sci.*, **21**, 409.
- CHAN, H.F. and G.O. WALKER (1984): Computer simulations of the ionospheric equatorial anomaly in East Asia for equinoctial, solar minimum conditions. Part II. Results and discussion of wind effects, *J. Atmos. Terr. Phys.*, **46**, 1113.
- HEDIN, A.E. (1986): MSIS86 thermospheric model, *J. Geophys. Res.*, **92**, 4649-4662.
- HEDIN, A.E. *et al.* (1991): Revised global models of thermosphere winds using satellite and ground-based observations, *J. Geophys. Res.*, **96**, 7657-7688.
- KILLEEN *et al.*, (1987): A computer model of global thermospheric wind and temperature, *Adv. Space Res.*, **7** (10), 207-215.
- MITRA, A.P. (1968): *J. Atmos. Terr. Phys.*, **30**, 1065-1114.
- ROBLE, R.G. *et al.* (1988): A coupled thermosphere/ionosphere general circulation model, *Geophys. Res. Lett.*, **15**, 1325-1328.
- RUSTER, R. (1971): *J. Atmos. Terr. Phys.*, **33**, 137.
- SOJKA, J.J. and R.W. SCHUNK (1985): A theoretical study of the global F region for June solstice, solar maximum and low magnetic activity, *J. Geophys. Res.*, **90**, 5285.
- STENING, R.J. (1992): Modelling the low latitude F region, *J. Atmos. Terr. Phys.*, **54** (11-12), 1387-1412.
- STROBEL, D.F. and T.R. YOUNG (1974): The night-time ionosphere: E region and lower F region, *J. Geophys. Res.*, **79**, 3171-3178.
- TORR, M.R. *et al.* (1979): *J. Geophys. Res.*, **84**, 3360-3379.
- WALKER, G.O. and H.F. CHAN (1989): Computer simulations of the seasonal variations of the ionospheric equatorial anomaly in East Asia under solar minimum conditions, *J. Atmos. Terr. Phys.*, **51**, 953-974.

(received May 25, 1993;
accepted August 23, 1993)